IMEX-REG: IMPLICIT-EXPLICIT REGULARIZATION IN THE FUNCTION SPACE FOR CONTINUAL LEARNING

Anonymous authors
Paper under double-blind review

ABSTRACT

Continual learning (CL) remains one of the long-standing challenges for deep neural networks due to catastrophic forgetting of previously acquired knowledge. Although rehearsal-based approaches have been fairly successful in mitigating catastrophic forgetting, they suffer from overfitting on buffered samples and prior information loss, hindering generalization under low-buffer regimes. Inspired by how humans learn using strong inductive biases, we propose **IMEX-Reg** to improve the generalization performance of experience rehearsal in CL under low buffer regimes. Specifically, we employ a two-pronged implicit-explicit regularization approach using contrastive representation learning (CRL) and consistency regularization. To further leverage the global relationship between representations learned using CRL, we propose a novel regularization strategy to guide the classifier toward the activation correlations in the unit hypersphere of the CRL. Our results show that IMEX-Reg significantly improves generalization performance and outperforms rehearsal-based approaches in several CL scenarios. It is also robust to natural and adversarial corruptions with less task-recency bias. Additionally, we provide theoretical insights to support our design decisions further. [1]

1 INTRODUCTION

Deep neural networks (DNNs) deployed in the real world frequently encounter dynamic data streams and must learn sequentially as the data becomes increasingly accessible over time (Parisi et al., 2019). However, continual learning (CL) over a sequence of tasks causes catastrophic forgetting (McCloskey & Cohen, 1989), a phenomenon in which acquiring new information disrupts consolidated knowledge, and in the worst case, the previously acquired information is completely forgotten. Rehearsal-based approaches (Aljundi et al., 2019; Buzzega et al., 2020; Arani et al., 2022) that maintain a bounded memory buffer to store and replay samples from previous tasks have been fairly effective in mitigating catastrophic forgetting. In practice, however, the buffer size is often limited due to memory constraints (such as on edge devices) and privacy concerns (e.g., GDPR). In such scenarios, repeated learning on bounded memory drastically reduces the ability of CL models to approximate past behavior, resulting in overfitting on buffered samples (Bhat et al., 2022a), exacerbated representation drift at the task boundary (Caccia et al., 2021) and prior information loss (Zhang et al., 2020), impeding generalization across tasks.

Humans, on the other hand, exhibit a remarkable ability to consolidate and transfer knowledge between distinct contexts in ever-changing environments (Barnett & Ceci, 2002), rarely interfering with consolidated knowledge (French, 1999). In the brain, CL is mediated by a plethora of neurophysiological processes that harbor strong inductive biases to encourage learning generalizable features, which require minimal adaptation when encountered with novel tasks. On the contrary, due to the lack of good inductive biases, DNNs often latch onto patterns that are only representative of the statistics of the training data (Sinz et al., 2019). Consequently, DNNs are typically susceptible to changes in the input distribution (Koh et al., 2021; Hendrycks et al., 2021). Therefore, leveraging inductive biases to incorporate prior knowledge in DNN can bias the learning process toward generalization.

Regularization has traditionally been used to introduce inductive bias in DNNs to prefer some hypotheses over others and promote generalization (Ruder, 2017). Multitask learning (MTL), a

---

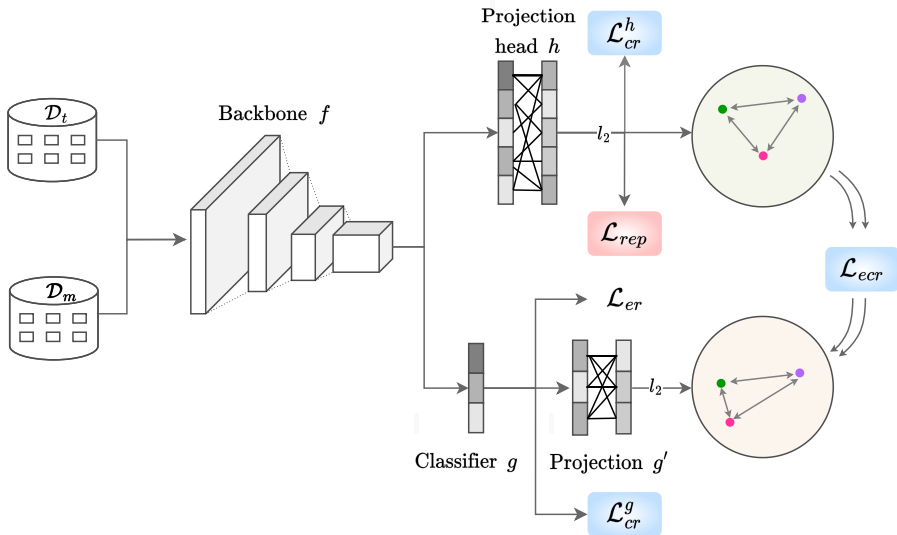[1]Code will be made publicly available upon acceptance.

Figure 1: Implicit - Explicit Regularization in CL: IMEX-Reg employs CRL ($\mathcal{L}_{rep}$) and consistency regularization ($\mathcal{L}_{cr}^g$ and $\mathcal{L}_{cr}^h$) to bias the learning towards generalization. To further leverage desirable traits of learning on unit-hypersphere using CRL, IMEX-Reg aligns the geometric structures within the classifier projection's hypersphere with that of the projection head's hypersphere ($\mathcal{L}_{ecr}$) thereby compensating for the weak supervision under low-buffer regimes.

form of inductive transfer that involves learning auxiliary tasks, acts as an implicit regularizer by introducing an inductive bias without imposing explicit constraints on the learning objective (Ruder, 2017). Sharing representations between related tasks in MTL helps DNNs to generalize better on the original task (Caruana, 1997). Moreover, assuming that the tasks in MTL share a common hypothesis class, sharing representations across tasks primarily benefits tasks with limited training samples (Liu et al., 2019). Contrastive representation learning (CRL) (Chen et al., 2020b; Khosla et al., 2020) as an auxiliary task in MTL promotes generalization in the shared parameters by maximizing the similarity between positive pairs and minimizing the similarity between negative pairs. A vast number of unsupervised CRL methods learn representations with a unit-norm constraint, effectively restricting the output space to the unit hypersphere (e.g. He et al. (2020)). Intuitively, having the features live on the unit hypersphere leads to several desirable traits: Fixed-norm vectors are known to improve training stability in modern machine learning where dot products are ubiquitous (Xu & Durrett, 2018). Moreover, if features of a class are sufficiently well clustered, they are linearly separable with the rest of the feature space (Wang & Isola, 2020). In addition to implicit regularization using CRL as an auxiliary task, the aforementioned desirable characteristics can be further leveraged for explicit classifier regularization, thereby compensating for weak supervision under low buffer regimes.

We propose IMEX-Reg, a two-pronged CL approach aimed at implicit regularization using hard parameter sharing and multi-task learning, and a novel explicit regularization in the function space to guide the optimization of the CL model towards generalization. Novelty in our method mainly lies in leveraging desirable traits of learning in the unit hypersphere through explicit classifier regularization in the function space. As CRL captures the global relationship between samples using instance discrimination tasks, we seek to align the geometric structures within the classifier hypersphere with those of the projection head hypersphere to compensate for the weak supervision under low buffer regimes. Our contributions are as follows:

- Inspired by how humans leverage inductive biases, we propose IMEX-Reg, a two pronged implicit-explicit regularization approach to mitigate catastrophic forgetting in CL.

- As having the features lie on the unit-hypersphere leads to several desirable traits, we propose a novel regularization strategy to guide the classifier toward the activation correlations in the unit-hypersphere of the CRL.

- We show that IMEX-Reg significantly improves generalization performance and outperforms rehearsal-based approaches in mitigating catastrophic forgetting in CL. IMEX-Reg is robust to natural and adversarial corruptions and well-calibrated with less task-recency bias.

- We also provide theoretical insights to support our design decisions better.

2 RELATED WORKS

Continual learning on a sequence of tasks with non-stationary data distributions results in catastrophic forgetting of older tasks, as training the CL model with new information interferes with previously consolidated knowledge (McClelland et al., 1995; Parisi et al., 2019). Experience-Rehearsal (ER) (Ratcliff, 1990; Robins, 1995) is one of the first works to address catastrophic forgetting by explicitly maintaining a memory buffer and interleaving previous task samples from the memory with the current task samples. Several works build on top of ER to reduce catastrophic forgetting further in CL under low buffer regimes. Deep Retrieval and Imagination (DRI) (Wang et al., 2022a) uses a generative model to produce additional (imaginary) data based on limited memory. ER-ACE (Caccia et al., 2022) focuses on preserving learned representations from drastic adaptations by combating representation drift under low buffer regimes. Gradient Coreset Replay (GCR) (Tiwari et al., 2022) proposes maintaining a coreset to select and update the memory buffer to leverage learning across tasks in a resource-efficient manner. Although rehearsal-based methods are fairly effective in challenging CL scenarios, they suffer from overfitting on buffered samples (Bhat et al., 2022a), exacerbated representation drift at the task boundary (Caccia et al., 2021), and prior information loss (Zhang et al., 2020) in low buffer regimes, thus hurting the generalizability of the model.

Regularization, implicit or explicit, is an important component in reducing the generalization error in DNNs. Although the parameter norm penalty is one way to regularize the CL model, parameter sharing using multitask learning (Caruana, 1997) can lead to better generalization and lower generalization error bounds if there is a valid statistical relationship between tasks (Baxter, 1995). Contrastive representation learning (Chen et al., 2020b; He et al., 2020; Henaff, 2020) that solves pretext prediction tasks to learn generalizable representations across a multitude of downstream tasks is an ideal candidate as an auxiliary task for implicit regularization. In CL, TARC (Bhat et al., 2022b) proposes a two-stage learning paradigm in which the model learns generalizable representations first using Supervised Contrastive (SupCon) (Khosla et al., 2020) loss followed by a modified supervised learning stage. Similarly, Co^2L (Cha et al., 2021) first learns representations using modified SupCon loss and then trains a classifier only on the last task samples and buffer data. However, these approaches require training in two phases and knowledge of the task boundary. OCDNet (Li et al., 2022) employs a student model and distills relational and adaptive knowledge using a modified SupCon objective. However, OCDNet does not leverage the generic information captured within the projection head to further reduce the overfitting of the classifier.

Explicit regularization in the function space imposes soft constraints on the parameters and optimizes the learning goal to converge upon a function that maps inputs to outputs. Therefore, several methods opt to directly limit how much the input/output function changes between tasks to promote generalization. Dark Experience Replay (DER++) (Buzzega et al., 2020) saves the model responses in the buffer and applies consistency regularization while replaying data from the memory buffer. Instead of storing the responses in the buffer, the Complementary Learning System-based ER (CLS-ER) (Arani et al., 2022) maintains dual semantic memories to enforce consistency regularization. However, in addition to consistency regularization, multitasking and explicit classifier regularization, in these approaches might enable further generalization in CL.

To this end, we propose to intertwine implicit and explicit regularization to promote generalization in CL under low buffer regimes. Novelty in our method mainly lies in leveraging generic representations learned within the projection head to compensate for weak supervision under low buffer regimes.

3 METHOD

Continual learning typically consists of $t \in \{1, 2, .., T\}$ sequence of tasks with the model learning one task at a time. Each task is specified by a task-specific data distribution $\mathcal{D}_t$ with $\{(x_i, y_i)\}_{i=1}^{N}$ pairs. Our CL model $\Phi_\theta = \{f, g, g', h\}$ consists of a shared backbone f, a linear classifier g, an

MLP classifier projection g', and a projection head h. The classifier g represents all the classes that belong to all the tasks, and the projection head h captures the embeddings of the ℓ_2-normalized representation. Classifier embeddings are further projected onto a unit hypersphere using another projection network g'. CL is especially challenging when data pertaining to previous tasks vanish as the CL model progresses to the next task. Therefore, to approximate the task-specific data distributions seen previously, we seek to maintain a memory buffer $\mathcal{D}_m$ using *Reservoir sampling* (Vitter, 1985) (Algorithm 2). To restrict the empirical risk on all tasks seen so far, ER minimizes the following objective:

$$\mathcal{L}_{er} = \frac{1}{|b|} \sum_{\substack{(x,y)\sim b \\ b \in \mathcal{D}_t \cup \mathcal{D}_m}} \mathcal{L}_{ce}(\sigma(g(f(x))), y) \tag{1}$$

where b is a training batch, $\mathcal{L}_{ce}$ is cross-entropy loss, t is the index of the current task, and $\sigma(.)$ is the softmax function. When the buffer size is limited, the CL model learns features specific to buffered samples rather than representative features that are class- or task-wide, resulting in poor performance on previously seen tasks. Therefore, we propose IMEX-Reg, aimed at implicit regularization using parameter sharing and multitask learning, and explicit regularization in the function space to guide the optimization of the CL model towards generalization. We describe in detail the different components of our approach in the following sections.

3.1 IMPLICIT REGULARIZATION

We seek to learn an auxiliary task that complements continual supervised learning. We consider CRL using SupCon (Khosla et al., 2020) loss as an auxiliary task to accumulate generalizable representations in shared parameters. Ideally, CRL involves highly correlated multiple augmented views of the same sample which are then propagated forward through the encoder f and the projection head h. To learn visual representations, the CL model should learn to maximize cosine similarity (ℓ_2-normalized dot product) between the positive pairs of multiple views while simultaneously pushing away the negative embeddings from the rest of the batch. The loss takes the following form:

$$\mathcal{L}_{rep} = \sum_{i \in I} \frac{-1}{|P(i)|} \sum_{p \in P(i)} [\ \langle \boldsymbol{z}_i \cdot \boldsymbol{z}_p \rangle / \tau - \log \sum_{n \in N(i)} \exp\left(\langle \boldsymbol{z}_i \cdot \boldsymbol{z}_n \rangle / \tau\right) \ ] \tag{2}$$

where $z = h(f(.))$ is any arbitrary 128-dimensional ℓ_2-normalized projection, τ is a temperature parameter, I is a set of b indices, $N(i) \equiv I \backslash \{i\}$ is a set of negative indices, $P(i) \equiv \{p \in N(i) : \boldsymbol{y}_p = \boldsymbol{y}_i\}$ is a set of projection indices that belong to the same class as the anchor z_i and $|P(i)|$ is its cardinality. In the following conjecture, we provide intuition behind choosing CRL as an auxiliary task in CL.

Conjecture 1. *(Feature similarity) Features learned by f through CRL are similar to those learned via cross-entropy as long as: (i) The augmentation in CRL do not corrupt semantic information, and (ii) The labels in cross-entropy rely mainly on this semantic information (Wen & Li, 2021).*

Let x_p^+ and x_p^{++} be two augmented positive samples such that $y_p^+ = y_p^{++}$. Furthermore, we assume that our raw data samples are generated in the following form: $x_p = \zeta_p + \xi_p$ where ζ_p represents semantic information in the image, while $\xi_p \sim \mathcal{D}_\xi = \mathcal{N}(0, \sigma)$ represents spurious noise. Given semantic preserving augmentations, (Wen & Li, 2021) state that similar discriminative features are learned by contrastive learning and cross-entropy. Similarly, since the CRL in Equation 2 employs both semantic preserving augmentations and labels to create positive pairs, we assume that the inner product of semantic information $\langle z_{\zeta_p^+}, z_{\zeta_p^{++}} \rangle$ will overwhelm that of the noisy signal $\langle z_{\xi_p^+}, z_{\xi_p^{++}} \rangle$. As we expect labels in cross-entropy to focus on semantic features to learn classification, we hypothesize that both CRL and cross-entropy share a common hypothesis class and sharing representations across these tasks especially benefits CL under low buffer regimes.

3.2 EXPLICIT REGULARIZATION

A CL model equipped with multitask learning implicitly encourages the shared encoder f to learn generalizable features. However, the classifier g that decides the final predictions is still prone to overfitting on buffered samples under low buffer regimes. Therefore, we seek to explicitly regularize the CL model in the function space defined by the classifier g. To this end, we denote the output

activation of the encoder f as $F \in \mathbb{R}^{b \times D_f}$, that of the projection head h as $Z \in \mathbb{R}^{b \times D_h}$, and that of the classifier projection g' as $C \in \mathbb{R}^{b \times D_g}$, where D_f, D_g, D_h denote the dimensions of output Euclidean spaces. Let $\mathcal{F}_g : \mathbb{R}^{D_f} \to \mathbb{R}^{D_g}$ and $\mathcal{F}_h : \mathbb{R}^{D_f} \to \mathbb{R}^{D_h}$ be the function spaces represented by the classifier g and the projection head h. Let θ and θ_{EMA} be parameters of the CL model and its corresponding exponential moving average (EMA). Following CLS-ER (Arani et al., 2022), we stochastically update the EMA model as follows:

$$\theta_{EMA} = \begin{cases} \eta\,\theta_{EMA} + (1 - \eta)\,\theta, & \text{if } \gamma \geq \mathcal{U}(0, 1) \\ \theta_{EMA}, & \text{otherwise} \end{cases} \tag{3}$$

where η is a decay parameter and γ is an update rate. The EMA of a model can be considered to form a self-ensemble of intermediate model states that leads to a better internal representation (Arani et al., 2022). Therefore, we leverage the soft targets (predictions) of the EMA model to regularize the learning trajectory in the function spaces $\mathcal{F}_g$ and $\mathcal{F}_h$ of the CL model:

$$\begin{aligned} \mathcal{L}_{cr}^g &\triangleq \mathbb{E}_{(x_j, y_j) \sim \mathcal{D}_m} \|\hat{y} - \hat{y}_e\|_F^2 \\ \mathcal{L}_{cr}^h &\triangleq \mathbb{E}_{(x_j, y_j) \sim \mathcal{D}_m} \|z - z_e\|_F^2 \end{aligned} \tag{4}$$

where $\|\cdot\|_F$ is the Frobenius norm, z and $\hat{y}$ are the projection head and classifier responses of the CL model, respectively, and z_e and $\hat{y}_e$ are those of the EMA model. As soft targets carry more information per training sample than ground truth labels (Hinton et al., 2015), knowledge of previous tasks can be better preserved by ensuring consistency in predictions, leading to drastic reductions in overfitting.

It is pertinent to note that restricting the output space to a unit hypersphere can improve training stability in representation learning (Wang & Isola, 2020). Moreover, well-clustered projections in the hypersphere are linearly separable from the rest of the samples. Therefore, regularizing the classifier using representations learned on a unit hypersphere can considerably reduce the generalization error. As semantically similar inputs tend to elicit similar responses, we seek to align geometric structures within the classifier's hypersphere with that of the projection head's hypersphere to further leverage global relationship between samples established using instance discrimination task. We assume that there exist a mapping function $\mathcal{M} : \mathbb{R}^{D_h} \to \mathbb{R}^{D_g}$ and its inverse $\mathcal{M}^{-1} : \mathbb{R}^{D_g} \to \mathbb{R}^{D_h}$ that establish a connection between the geometric relationship between the points in both hyperspheres. When learning in the hypersphere, angular information rather than magnitude forms the key semantics in the CL model (Chen et al., 2020a). Therefore, to guide the classifier toward the activation correlations in the unit hypersphere of the projection head, we regularize the differences in the outer products of Z and C, i.e.,

$$\begin{aligned} G_h &= ZZ^T \in \mathbb{R}^{b,b} \\ G_g &= CC^T \in \mathbb{R}^{b,b} \end{aligned} \tag{5}$$

$$\mathcal{L}_{ecr} = \frac{1}{|b|^2} \|stopgrad(G_h) - G_g\|_F^2 \tag{6}$$

where $stopgrad(.)$ ensures that the backpropagation of gradients occurs only through the classifier. Equation 4 regularizes both the classifier and the projection head using the EMA of the CL model, while $\mathcal{L}_{ecr}$ in Equation 6 captures the mean element-wise squared difference between G_h and G_g matrices of the CL model.

Johnson-Lindenstrauss (JL) lemma (Dasgupta & Gupta, 2003) states that any p points in a high dimensional Euclidean space can be mapped onto k dimensions where $k \geq O\left(\log p/\epsilon^2\right)$ without distorting the Euclidean distance between any two points more than a factor of $1 \pm \epsilon$. Under JL lemma, we hypothesize that it is possible to map geometric relationship between points in a higher dimensional projection head hypersphere to a lower dimensional classifier hypersphere without the loss of generality. To this end, we propose a novel mapping function $\mathcal{L}_{ecr}$ that preserves the geometric structures when mapping from projection head to classifier. Application of JL lemma in this context implies that the distortion in geometric relationship between points when mapping from projection head to classifier hypersphere can be limited to $1 \pm \epsilon$. More details about JL lemma can be found in Theorem 2 in Appendix A.

Algorithm 1 Proposed Method: IMEX-Reg

1: **Input:** Data streams $\mathcal{D}_t$, Model $\Phi_\theta = \{f, g, g', h\}$, Hyperparameters α, β and λ, Memory buffer $\mathcal{D}_m \leftarrow \{\}$
2: **for all** tasks $t \in \{1, 2, .., T\}$ **do**
3:     **for all** Iterations $e \in \{1, 2, .., E\}$ **do**
4:         $\mathcal{L} = 0$
5:         Sample a minibatch $(X_t, Y_t) \in \mathcal{D}_t$
6:         $F_t = f(X_t)$
7:         $\hat{Y}_t, Z_t, C_t = g(F_t), h(F_t), g'(g(F_t))$
8:         **if** $\mathcal{D}_m \neq \emptyset$ **then**
9:             Sample a minibatch $(X_m, Y_m) \in \mathcal{D}_m$
10:            $F_m = f(X_m)$
11:            $\hat{Y}, Z, C = g(F_m), h(F_m), g'(g(F_m))$
12:            $F_e = f_e(X_m)$
13:            $\hat{Y}_e, Z_e, C_e = g_e(F_m), h_e(F_m), g'_e(g_e(F_m))$
14:            $\mathcal{L} \mathrel{+}= \lambda \left[\mathcal{L}_{cr}^g + \mathcal{L}_{cr}^h \right]$
15:         $\mathcal{L} \mathrel{+}= \mathcal{L}_{er} + \alpha\, \mathcal{L}_{rep} + \beta\, \mathcal{L}_{ecr}$
16:         Update Φ_θ and $\mathcal{D}_m$
17:         Update θ_{ema}
18: **return** model Φ_θ

3.3 PUTTING IT ALL TOGETHER

During training, the batches of the current task are propagated forward through Φ_θ to obtain classification and projection embeddings. Specifically, Φ_θ learns generalizable features through Equation 2 and task-specific features through Equation 1. To better consolidate the information pertaining to previous tasks, we maintain a memory buffer $\mathcal{D}_m$ and an EMA of the CL model, which also serves as an inference model for evaluation. We enforce consistency in predictions on rehearsal data using Equation 4. To further reduce overfitting and discourage label bias in the classifier, we seek to emulate geometric structures using Equation 6. During each training iteration, the memory buffer is updated using Reservoir sampling (Vitter, 1985) and the EMA is stochastically updated using Equation 3. The overall learning objective is as follows:

$$\mathcal{L} \triangleq \mathop{\mathbb{E}}_{(x,y) \sim \mathcal{D}_t \cup \mathcal{D}_m} \left[\mathcal{L}_{er} + \alpha\, \mathcal{L}_{rep} + \beta\, \mathcal{L}_{ecr} \right] + \mathop{\mathbb{E}}_{(x,y) \sim \mathcal{D}_m} \lambda \left[\mathcal{L}_{cr}^g + \mathcal{L}_{cr}^h \right] \tag{7}$$

where α, β and λ are hyperparameters. IMEX-Reg is illustrated in Figure 1 and is detailed in Algorithm 1. Novelty in IMEX-Reg mainly lies in leveraging generic representations learned within the projection head to compensate for weak supervision under low buffer regimes.

4 EXPERIMENTS

4.1 EXPERIMENTAL SETUP

We build on top of the Mammoth (Buzzega et al., 2020) CL repository in PyTorch. We evaluate CL models under Class-Incremental Learning (Class-IL), Task-Incremental Learning (Task-IL), and Generalized Class-IL (GCIL) (Van de Ven & Tolias, 2019; Arani et al., 2022). More information on the datasets, task partition, and the corresponding network architecture used in these scenarios can be found in Appendix E. To provide a comprehensive analysis, we compare IMEX-Reg with several approaches that aim to improve generalization under low buffer regimes in CL. We consider ER-ACE, GCR, DRI (aimed at improving generalization), DER++, CLS-ER (use explicit consistency regularization by leveraging soft targets), Co^{2}L and OCDNet (representation and/or auxiliary CRL) as our baselines. Furthermore, we provide a lower bound 'SGD', without using any mechanism to minimize catastrophic forgetting, and an upper bound 'Joint', where the training is carried out using the entire dataset. We report the average accuracy along with standard deviation on all tasks after CL training with three random seeds. We also provide the results of the forgetting analysis in Appendix C.1.

Table 1: Top-1 accuracy (%) of different CL models in Class-IL and Task-IL scenarios with varying complexities and memory buffer sizes. The best results are marked in bold.

Buffer	Methods	Venue	Seq-CIFAR10		Seq-CIFAR100		Seq-TinyImageNet	
			Class-IL	Task-IL	Class-IL	Task-IL	Class-IL	Task-IL
-	SGD	-	$19.62_{\pm0.05}$	$61.02_{\pm3.33}$	$17.49_{\pm0.28}$	$40.46_{\pm0.99}$	$07.92_{\pm0.26}$	$18.31_{\pm0.68}$
	Joint	-	$92.20_{\pm0.15}$	$98.31_{\pm0.12}$	$70.56_{\pm0.28}$	$86.19_{\pm0.43}$	$59.99_{\pm0.19}$	$82.04_{\pm0.10}$
200	ER	-	$44.79_{\pm1.86}$	$91.19_{\pm0.94}$	$21.40_{\pm0.22}$	$61.36_{\pm0.35}$	$8.57_{\pm0.04}$	$38.17_{\pm2.00}$
	ER-ACE	ICLR'22	$62.08_{\pm1.44}$	$92.20_{\pm0.57}$	$35.17_{\pm1.17}$	$63.09_{\pm1.23}$	$11.25_{\pm0.54}$	$44.17_{\pm1.02}$
	GCR	CVPR'22	$64.84_{\pm1.63}$	$90.8_{\pm1.05}$	$33.69_{\pm1.40}$	$64.24_{\pm0.83}$	$13.05_{\pm0.91}$	$42.11_{\pm1.01}$
	DRI	AAAI'22	$65.16_{\pm1.13}$	$92.87_{\pm0.71}$	-	-	$17.58_{\pm1.24}$	$44.28_{\pm1.37}$
	DER++	NeurIPS'20	$64.88_{\pm1.17}$	$91.92_{\pm0.60}$	$29.60_{\pm1.14}$	$62.49_{\pm1.02}$	$10.96_{\pm1.17}$	$40.87_{\pm1.16}$
	CLS-ER	ICLR'22	$66.19_{\pm0.75}$	$93.90_{\pm0.60}$	$43.80_{\pm1.89}$	$73.49_{\pm1.04}$	$23.47_{\pm0.80}$	$49.60_{\pm0.72}$
	Co^{2}L	ICCV'21	$65.57_{\pm1.37}$	$93.43_{\pm0.78}$	$31.90_{\pm0.38}$	$55.02_{\pm0.36}$	$13.88_{\pm0.40}$	$42.37_{\pm0.74}$
	OCDNet	IJCAI'22	$\mathbf{73.38}_{\pm0.32}$	$\mathbf{95.43}_{\pm0.30}$	$44.29_{\pm0.49}$	$73.53_{\pm0.24}$	$17.60_{\pm0.97}$	$56.19_{\pm1.31}$
	IMEX-Reg	-	$71.56_{\pm0.18}$	$94.77_{\pm0.81}$	$\mathbf{48.54}_{\pm0.23}$	$\mathbf{75.61}_{\pm0.73}$	$\mathbf{24.15}_{\pm0.78}$	$\mathbf{62.91}_{\pm0.54}$
500	ER	-	$57.74_{\pm0.27}$	$93.61_{\pm0.27}$	$28.02_{\pm0.31}$	$68.23_{\pm0.17}$	$9.99_{\pm0.29}$	$48.64_{\pm0.46}$
	ER-ACE	ICLR'22	$68.45_{\pm1.78}$	$93.47_{\pm1.00}$	$40.67_{\pm0.06}$	$66.45_{\pm0.71}$	$17.73_{\pm0.56}$	$49.99_{\pm1.51}$
	GCR	CVPR'22	$74.69_{\pm0.85}$	$94.44_{\pm0.32}$	$45.91_{\pm1.30}$	$71.64_{\pm2.10}$	$19.66_{\pm0.68}$	$52.99_{\pm0.89}$
	DRI	AAAI'22	$72.78_{\pm1.44}$	$93.85_{\pm0.46}$	-	-	$22.63_{\pm0.81}$	$52.89_{\pm0.60}$
	DER++	NeurIPS'20	$72.70_{\pm1.36}$	$93.88_{\pm0.50}$	$41.40_{\pm0.96}$	$70.61_{\pm0.08}$	$19.38_{\pm1.41}$	$51.91_{\pm0.68}$
	CLS-ER	ICLR'22	$75.22_{\pm0.71}$	$94.94_{\pm0.53}$	$51.40_{\pm1.00}$	$78.12_{\pm0.24}$	$31.03_{\pm0.56}$	$60.41_{\pm0.50}$
	Co^{2}L	ICCV'21	$74.26_{\pm0.77}$	$95.90_{\pm0.26}$	$39.21_{\pm0.39}$	$62.98_{\pm0.58}$	$20.12_{\pm0.42}$	$53.04_{\pm0.69}$
	OCDNet	IJCAI'22	$\mathbf{80.64}_{\pm0.77}$	$\mathbf{96.57}_{\pm0.07}$	$54.13_{\pm0.36}$	$78.51_{\pm0.24}$	$26.09_{\pm0.28}$	$64.76_{\pm0.29}$
	IMEX-Reg	-	$77.61_{\pm0.18}$	$95.96_{\pm0.33}$	$\mathbf{56.53}_{\pm0.80}$	$\mathbf{80.51}_{\pm0.10}$	$\mathbf{31.41}_{\pm0.21}$	$\mathbf{67.44}_{\pm0.38}$

4.2 EXPERIMENTAL RESULTS

Table 1 presents the comparison of our method with the baselines for the Class-IL and Task-IL settings. Several observations can be made from these results: (i) Although CL methods aimed at generalization improve over ER, they lack strong inductive biases proposed in this work, thus failing to make significant improvements in low-buffer regimes. (ii) Explicit consistency regularization shows great promise in reducing overfitting over ER. As can be seen, DER++, DRI, and CLS-ER show significant reductions in catastrophic forgetting compared to ER. However, IMEX-Reg incorporates implicit and explicit regularization to promote generalization and outperforms these methods by a large margin in most scenarios. In Seq-TinyImageNet, IMEX-Reg outperforms CLS-ER by a relative margin of 2.9% and 1.2% in buffer sizes 200 and 500, respectively. Note that CLS-ER employs two semantic memories, while IMEX-Reg uses only one.

Co^{2}L and OCDNet generalize well across tasks in CL, showing the efficacy of CRL in CL. Specifically, OCDNet combines consistency regularization and CRL in addition to self-supervised rotation prediction. OCDNet outperforms IMEX-Reg in Seq-CIFAR10 in both buffer sizes, greatly benefiting from rotation prediction. However, OCDNet lags behind IMEX-Reg by a large margin in more challenging datasets. Essentially, IMEX-Reg compensates the classifier's weak supervision with the generic geometric structures learned by the projection head through a novel explicit regularization, achieving a relative 9.6% and 37.22% improvement over OCDNet in Seq-CIFAR100 and Seq-TinyImageNet, respectively, for a low buffer size of 200. This reinforces our earlier hypothesis in Conjecture 1 that leveraging desirable traits from CRL can indeed guide the classifier towards generalization under low buffer regimes.

Generalized Class-IL (GCIL) exposes the CL model to a more challenging and realistic learning scenario by using probabilistic distributions to sample data from the CIFAR100 dataset in each task (Mi et al., 2020). Table 2 shows the comparison of different CL methods in GCIL setting under two variations, Uniform and Longtail (class imbalance). As can be seen, IMEX-Reg outperforms all the baselines by a large margin across all buffer sizes. IMEX-Reg performs significantly better than ER, ER-ACE, DER++ and CLS-ER, emphasizing the importance of implicit regularization through auxiliary CRL in improving generalization. Although OCDNet combines auxiliary CRL and explicit consistency regularization, OCDNet falls behind IMEX-Reg by a considerable margin across all GCIL scenarios. Even under class imbalance (Longtail) and a low buffer size of 100, IMEX-Reg achieves a relative improvement of 7.8% over OCDNet. These results indicate that IMEX-Reg

Table 2: Top-1 accuracy (%) of different CL models for Uniform and Longtail GCIL-CIFAR100 settings with different memory buffer sizes. The best results are marked in bold.

Method	Uniform			Longtail		
SGD		10.38 ± 0.26			9.61 ± 0.19	
Joint		58.59 ± 1.95			58.42 ± 1.32	
Buffer	100	200	500	100	200	500
ER	14.43 ± 0.36	16.52 ± 0.10	23.62 ± 0.66	13.22 ± 0.6	16.20 ± 0.30	22.36 ± 1.27
ER-ACE	23.76 ± 1.61	27.64 ± 0.76	30.14 ± 1.11	23.05 ± 0.18	25.10 ± 2.64	31.88 ± 0.73
DER++	21.17 ± 1.65	27.73 ± 0.93	35.83 ± 0.62	20.29 ± 1.03	26.48 ± 2.07	34.23 ± 1.19
CLS-ER	33.42 ± 0.30	35.88 ± 0.41	38.94 ± 0.38	33.92 ± 0.79	35.67 ± 0.72	38.79 ± 0.67
OCDNet	37.21 ± 0.69	39.94 ± 0.05	43.58 ± 0.67	35.61 ± 1.13	39.97 ± 0.70	43.57 ± 0.23
IMEX-Reg	$\mathbf{39.48}\pm0.25$	$\mathbf{43.19}\pm0.47$	$\mathbf{49.07}\pm0.59$	$\mathbf{38.39}\pm0.46$	$\mathbf{42.66}\pm0.82$	$\mathbf{46.81}\pm1.04$

learns generalizable features through auxiliary CRL while enriching the classifier through explicit regularization in the function space, making it suitable for challenging CL scenarios.

4.3 ABLATION STUDY

We seek to provide a better understanding of the contributions of each of the components in our proposed method. Table 3 shows the ablation study of IMEX-Reg trained on Seq-CIFAR100 for a buffer size of 200 with 5 tasks. In line with our earlier hypothesis, intertwining implicit regularization using parameter sharing and multitask learning, and explicit regularization in the function space guides the optimization of the IMEX-Reg towards better generalization representations. As can be seen, each of these components has a significant impact on the performance of IMEX-Reg under a low buffer regime. Additionally, leveraging generic geometric structures learned within CRL through a novel explicit classifier regularization complements weak supervision under low buffer regimes and results in lower generalization error.

Table 3: Comparison of the contributions of each of the components in IMEX-Reg. The absence of EMA implies consistency regularization by storing past logits.

$\mathcal{L}_{cr}$	EMA	$\mathcal{L}_{rep}$	$\mathcal{L}_{ecr}$	Accuracy
✓	✓	✓	✓	$\mathbf{48.54}\pm0.23$
✓	✓	✓	✗	46.85 ± 0.48
✓	✓	✗	✗	43.38 ± 1.06
✓	✗	✗	✗	29.60 ± 1.14
✗	✗	✗	✗	21.40 ± 0.22

5 MODEL CHARACTERISTICS

Task Recency Bias. Learning continuously on a sequence of tasks biases the model predictions toward recently learned tasks in the Class-IL scenario (Hou et al., 2019). An ideal CL model is expected to have the least bias, with predictions evenly distributed across all tasks. To gauge the task-recency bias in IMEX-Reg, we compute the average task probabilities by averaging the softmax outputs of all samples associated with each task on the test set at the end of the training. Figure 2(right) shows the task-recency bias of different CL models trained on Seq-CIFAR100 with buffer size 200. Evidently, IMEX-Reg predictions are more evenly distributed with least recency bias. IMEX-Reg induces robust inductive biases that skew the learning process towards generic representations instead of aligning more with the current task, thereby reducing recency bias.

Robustness to Adversarial Attacks. Adversarial attacks generate specially crafted images with imperceptible perturbations to fool the network into making false predictions (Szegedy et al., 2013). We analyze adversarial robustness by performing a PGD-10 attack (Madry et al., 2017) with varying attack intensities on different models trained on Seq-CIFAR100 with a buffer size of 200. Figure 2(left) shows that IMEX-Reg is more resistant to adversarial attacks compared to other baselines. OCDNet and IMEX-Reg are significantly more robust than DER++ and ER even at higher attack intensities, owing to the auxiliary CRL that encourages the model to learn generalizable features. However, IMEX-Reg further biases the model towards generalization through the novel explicit classifier regularization and outperforms OCDNet across all attack intensities. Thus, inducing right-
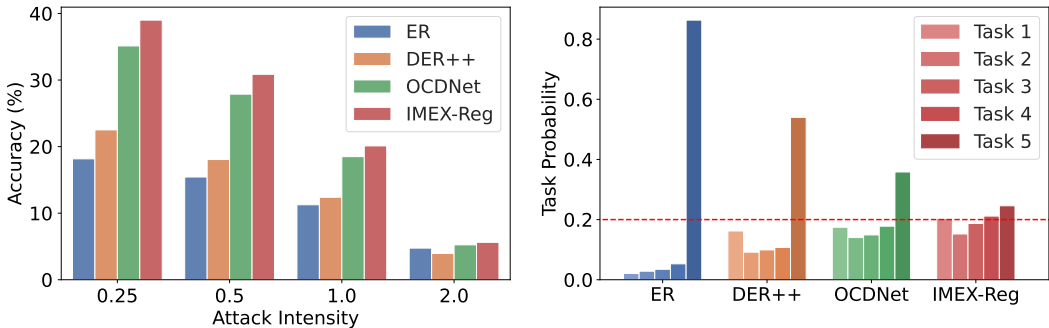
Figure 2: (Left) Robustness to PGD adversarial attack at varying strengths and (Right) Average probability of predicting each task for different CL methods trained on Seq-CIFAR100 with 5 tasks. IMEX-Reg shows the highest robustness and the least recency bias with probabilities evenly distributed across tasks.

inductive biases in the model can improve the robustness of the model in addition to improved performance.

Robustness to Natural Corruptions: Data in the wild is often corrupted by changes in illumination, digital imaging artifacts, or weather conditions. Therefore, autonomous agents deployed in the real world should be robust to these natural corruptions, especially in safety-critical applications. To evaluate the robustness to natural corruptions, we test several CL methods trained on Seq-CIFAR00 with buffer size 500 on CIFAR100-C (Hendrycks & Dietterich, 2019). Figure 3 shows the accuracy of different CL models compared to IMEX-Reg for 19 different corruptions averaged at five severity levels. Although OCDNet combines knowledge distillation and CRL, it is unable to improve its robustness over DER++. However, IMEX-Reg further enriches the classifier with the generic geometric structures learned in the projection head, proving to be more robust to natural corruptions.

Additional information such as theoretical background A, broader related works B, characteristic analysis C, limitations and broader impact D and implementation details E can be found in the Appendix.
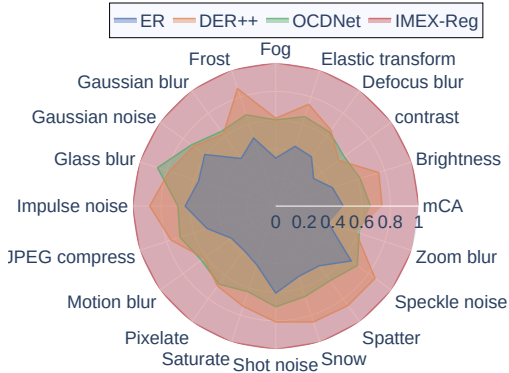

Figure 3: Relative top-1 accuracy (%) (averaged over 5 severity levels) for 19 different natural corruptions for different CL models trained on Seq-CIFAR100 with 5 tasks. The average accuracy across all corruptions is shown as mCA.

6 CONCLUSION

We propose IMEX-Reg, a two-pronged CL approach aimed at implicit regularization using hard parameter sharing and multitask learning, and a novel explicit regularization in the function space to guide the optimization of the CL model towards generalization. Novelty in our method mainly lies in emulating rich geometric structures learned within the projection head hypersphere to compensate for weak supervision under low buffer regimes. Through extensive experimental evaluation, we show that IMEX-Reg significantly benefits from each of these strong inductive biases and exhibits strong performance across several CL scenarios. Furthermore, we show that IMEX-Reg is robust and mitigates task recency bias. Leveraging unlabeled data through CRL in IMEX-Reg could further improve generalization performance across tasks in CL.

REFERENCES

Rahaf Aljundi, Min Lin, Baptiste Goujaud, and Yoshua Bengio. Gradient based sample selection for online continual learning. In H. Wallach, H. Larochelle, A. Beygelzimer, F. d'Alché-Buc, E. Fox, and R. Garnett (eds.), *Advances in Neural Information Processing Systems*, volume 32. Curran Associates, Inc., 2019.

Elahe Arani, Fahad Sarfraz, and Bahram Zonooz. Learning fast, learning slow: A general continual learning method based on complementary learning system. In *International Conference on Learning Representations*, 2022.

Jihwan Bang, Heesu Kim, YoungJoon Yoo, Jung-Woo Ha, and Jonghyun Choi. Rainbow memory: Continual learning with a memory of diverse samples. In *Proceedings of the IEEE/CVF conference on computer vision and pattern recognition*, pp. 8218–8227, 2021.

Susan M Barnett and Stephen J Ceci. When and where do we apply what we learn?: A taxonomy for far transfer. *Psychological bulletin*, 128(4):612, 2002.

Jonathan Baxter. Learning internal representations. In *Proceedings of the eighth annual conference on Computational learning theory*, pp. 311–320, 1995.

Prashant Shivaram Bhat, Bahram Zonooz, and Elahe Arani. Consistency is the key to further mitigating catastrophic forgetting in continual learning. In *Conference on Lifelong Learning Agents*, pp. 1195–1212. PMLR, 2022a.

Prashant Shivaram Bhat, Bahram Zonooz, and Elahe Arani. Task agnostic representation consolidation: a self-supervised based continual learning approach. In *Conference on Lifelong Learning Agents*, pp. 390–405. PMLR, 2022b.

Lorenzo Bonicelli, Matteo Boschini, Angelo Porrello, Concetto Spampinato, and Simone Calderara. On the effectiveness of lipschitz-driven rehearsal in continual learning. *Advances in Neural Information Processing Systems*, 35:31886–31901, 2022.

Matteo Boschini, Pietro Buzzega, Lorenzo Bonicelli, Angelo Porrello, and Simone Calderara. Continual semi-supervised learning through contrastive interpolation consistency. *Pattern Recognition Letters*, 162:9–14, 2022.

Pietro Buzzega, Matteo Boschini, Angelo Porrello, Davide Abati, and Simone Calderara. Dark experience for general continual learning: a strong, simple baseline. In H. Larochelle, M. Ranzato, R. Hadsell, M. F. Balcan, and H. Lin (eds.), *Advances in Neural Information Processing Systems*, volume 33, pp. 15920–15930. Curran Associates, Inc., 2020.

Lucas Caccia, Rahaf Aljundi, Nader Asadi, Tinne Tuytelaars, Joelle Pineau, and Eugene Belilovsky. Reducing representation drift in online continual learning. *arXiv preprint arXiv:2104.05025*, 2021.

Lucas Caccia, Rahaf Aljundi, Nader Asadi, Tinne Tuytelaars, Joelle Pineau, and Eugene Belilovsky. New insights on reducing abrupt representation change in online continual learning. In *International Conference on Learning Representations*, 2022.

Rich Caruana. Multitask learning. *Machine learning*, 28:41–75, 1997.

Hyuntak Cha, Jaeho Lee, and Jinwoo Shin. Co2l: Contrastive continual learning. In *Proceedings of the IEEE/CVF International Conference on Computer Vision*, pp. 9516–9525, 2021.

Arslan Chaudhry, Puneet K Dokania, Thalaiyasingam Ajanthan, and Philip HS Torr. Riemannian walk for incremental learning: Understanding forgetting and intransigence. In *Proceedings of the European Conference on Computer Vision (ECCV)*, pp. 532–547, 2018.

Beidi Chen, Weiyang Liu, Zhiding Yu, Jan Kautz, Anshumali Shrivastava, Animesh Garg, and Animashree Anandkumar. Angular visual hardness. In *International Conference on Machine Learning*, pp. 1637–1648. PMLR, 2020a.

Ting Chen, Simon Kornblith, Mohammad Norouzi, and Geoffrey Hinton. A simple framework for contrastive learning of visual representations. In *International conference on machine learning*, pp. 1597–1607. PMLR, 2020b.

Hong-Jun Choi and Dong-Wan Choi. Attractive and repulsive training to address inter-task forgetting issues in continual learning. *Neurocomputing*, 500:486–498, 2022.

Sanjoy Dasgupta and Anupam Gupta. An elementary proof of a theorem of Johnson and Lindenstrauss. *Random Structures & Algorithms*, 22(1):60–65, 2003.

Robert M French. Catastrophic forgetting in connectionist networks. *Trends in cognitive sciences*, 3 (4):128–135, 1999.

Chuan Guo, Geoff Pleiss, Yu Sun, and Kilian Q Weinberger. On calibration of modern neural networks. In *International conference on machine learning*, pp. 1321–1330. PMLR, 2017.

Kaiming He, Haoqi Fan, Yuxin Wu, Saining Xie, and Ross Girshick. Momentum contrast for unsupervised visual representation learning. In *Proceedings of the IEEE/CVF conference on computer vision and pattern recognition*, pp. 9729–9738, 2020.

Olivier Henaff. Data-efficient image recognition with contrastive predictive coding. In *International conference on machine learning*, pp. 4182–4192. PMLR, 2020.

Dan Hendrycks and Thomas Dietterich. Benchmarking neural network robustness to common corruptions and perturbations. *Proceedings of the International Conference on Learning Representations*, 2019.

Dan Hendrycks, Steven Basart, Norman Mu, Saurav Kadavath, Frank Wang, Evan Dorundo, Rahul Desai, Tyler Zhu, Samyak Parajuli, Mike Guo, et al. The many faces of robustness: A critical analysis of out-of-distribution generalization. In *Proceedings of the IEEE/CVF International Conference on Computer Vision*, pp. 8340–8349, 2021.

Geoffrey Hinton, Oriol Vinyals, Jeff Dean, et al. Distilling the knowledge in a neural network. *arXiv preprint arXiv:1503.02531*, 2(7), 2015.

Saihui Hou, Xinyu Pan, Chen Change Loy, Zilei Wang, and Dahua Lin. Learning a unified classifier incrementally via rebalancing. In *Proceedings of the IEEE/CVF conference on computer vision and pattern recognition*, pp. 831–839, 2019.

Xisen Jin, Arka Sadhu, Junyi Du, and Xiang Ren. Gradient-based editing of memory examples for online task-free continual learning. *Advances in Neural Information Processing Systems*, 34: 29193–29205, 2021.

Prannay Khosla, Piotr Teterwak, Chen Wang, Aaron Sarna, Yonglong Tian, Phillip Isola, Aaron Maschinot, Ce Liu, and Dilip Krishnan. Supervised contrastive learning. *Advances in Neural Information Processing Systems*, 33:18661–18673, 2020.

Gyuhak Kim, Changnan Xiao, Tatsuya Konishi, Zixuan Ke, and Bing Liu. A theoretical study on solving continual learning. *Advances in Neural Information Processing Systems*, 35:5065–5079, 2022.

Jong-Yeong Kim and Dong-Wan Choi. Split-and-bridge: Adaptable class incremental learning within a single neural network. In *Proceedings of the AAAI Conference on Artificial Intelligence*, volume 35, pp. 8137–8145, 2021.

Pang Wei Koh, Shiori Sagawa, Henrik Marklund, Sang Michael Xie, Marvin Zhang, Akshay Balsubramani, Weihua Hu, Michihiro Yasunaga, Richard Lanas Phillips, Irena Gao, et al. Wilds: A benchmark of in-the-wild distribution shifts. In *International Conference on Machine Learning*, pp. 5637–5664. PMLR, 2021.

Fabian Küppers, Jan Kronenberger, Amirhossein Shantia, and Anselm Haselhoff. Multivariate confidence calibration for object detection. In *The IEEE/CVF Conference on Computer Vision and Pattern Recognition (CVPR) Workshops*, June 2020.

Timothée Lesort, Andrei Stoian, and David Filliat. Regularization shortcomings for continual learning. *arXiv preprint arXiv:1912.03049*, 2019.

Jin Li, Zhong Ji, Gang Wang, Qiang Wang, and Feng Gao. Learning from students: Online contrastive distillation network for general continual learning. In Lud De Raedt (ed.), *Proceedings of the Thirty-First International Joint Conference on Artificial Intelligence, IJCAI-22*, pp. 3215–3221. International Joint Conferences on Artificial Intelligence Organization, 7 2022.

Xiaodong Liu, Pengcheng He, Weizhu Chen, and Jianfeng Gao. Multi-task deep neural networks for natural language understanding. In *Proceedings of the 57th Annual Meeting of the Association for Computational Linguistics*, pp. 4487–4496, 2019.

Aleksander Madry, Aleksandar Makelov, Ludwig Schmidt, Dimitris Tsipras, and Adrian Vladu. Towards deep learning models resistant to adversarial attacks. *arXiv preprint arXiv:1706.06083*, 2017.

Avner Magen. Dimensionality reductions that preserve volumes and distance to affine spaces, and their algorithmic applications. In *International Workshop on Randomization and Approximation Techniques in Computer Science*, pp. 239–253. Springer, 2002.

James L McClelland, Bruce L McNaughton, and Randall C O'Reilly. Why there are complementary learning systems in the hippocampus and neocortex: insights from the successes and failures of connectionist models of learning and memory. *Psychological review*, 102(3):419, 1995.

Michael McCloskey and Neal J Cohen. Catastrophic interference in connectionist networks: The sequential learning problem. In *Psychology of learning and motivation*, volume 24, pp. 109–165. Elsevier, 1989.

Fei Mi, Lingjing Kong, Tao Lin, Kaicheng Yu, and Boi Faltings. Generalized class incremental learning. In *Proceedings of the IEEE/CVF Conference on Computer Vision and Pattern Recognition Workshops*, pp. 240–241, 2020.

German I Parisi, Ronald Kemker, Jose L Part, Christopher Kanan, and Stefan Wermter. Continual lifelong learning with neural networks: A review. *Neural Networks*, 113:54–71, 2019.

Roger Ratcliff. Connectionist models of recognition memory: constraints imposed by learning and forgetting functions. *Psychological review*, 97(2):285, 1990.

Anthony Robins. Catastrophic forgetting, rehearsal and pseudorehearsal. *Connection Science*, 7(2): 123–146, 1995.

Sebastian Ruder. An overview of multi-task learning in deep neural networks. *arXiv preprint arXiv:1706.05098*, 2017.

Fahad Sarfraz, Elahe Arani, and Bahram Zonooz. Synergy between synaptic consolidation and experience replay for general continual learning. In Sarath Chandar, Razvan Pascanu, and Doina Precup (eds.), *Proceedings of The 1st Conference on Lifelong Learning Agents*, volume 199 of *Proceedings of Machine Learning Research*, pp. 920–936. PMLR, 22–24 Aug 2022.

Fabian H Sinz, Xaq Pitkow, Jacob Reimer, Matthias Bethge, and Andreas S Tolias. Engineering a less artificial intelligence. *Neuron*, 103(6):967–979, 2019.

Christian Szegedy, Wojciech Zaremba, Ilya Sutskever, Joan Bruna, Dumitru Erhan, Ian Goodfellow, and Rob Fergus. Intriguing properties of neural networks. *arXiv preprint arXiv:1312.6199*, 2013.

Rishabh Tiwari, Krishnateja Killamsetty, Rishabh Iyer, and Pradeep Shenoy. Gcr: Gradient coreset based replay buffer selection for continual learning. In *Proceedings of the IEEE/CVF Conference on Computer Vision and Pattern Recognition*, pp. 99–108, 2022.

Gido M Van de Ven and Andreas S Tolias. Three scenarios for continual learning. *arXiv preprint arXiv:1904.07734*, 2019.

Eli Verwimp, Matthias De Lange, and Tinne Tuytelaars. Rehearsal revealed: The limits and merits of revisiting samples in continual learning. In *Proceedings of the IEEE/CVF International Conference on Computer Vision*, pp. 9385–9394, 2021.

Jeffrey S Vitter. Random sampling with a reservoir. *ACM Transactions on Mathematical Software (TOMS)*, 11(1):37–57, 1985.

Tongzhou Wang and Phillip Isola. Understanding contrastive representation learning through alignment and uniformity on the hypersphere. In *International Conference on Machine Learning*, pp. 9929–9939. PMLR, 2020.

Zhen Wang, Liu Liu, Yiqun Duan, and Dacheng Tao. Continual learning through retrieval and imagination. In *AAAI Conference on Artificial Intelligence*, volume 8, 2022a.

Zhenyi Wang, Li Shen, Le Fang, Qiuling Suo, Tiehang Duan, and Mingchen Gao. Improving task-free continual learning by distributionally robust memory evolution. In *International Conference on Machine Learning*, pp. 22985–22998. PMLR, 2022b.

Zixin Wen and Yuanzhi Li. Toward understanding the feature learning process of self-supervised contrastive learning. In *International Conference on Machine Learning*, pp. 11112–11122. PMLR, 2021.

Jiacheng Xu and Greg Durrett. Spherical latent spaces for stable variational autoencoders. In *Proceedings of the 2018 Conference on Empirical Methods in Natural Language Processing*, pp. 4503–4513, 2018.

Song Zhang, Gehui Shen, Jinsong Huang, and Zhi-Hong Deng. Self-supervised learning aided class-incremental lifelong learning. *arXiv preprint arXiv:2006.05882*, 2020.

A   Theoretical Background

Theorem 2. *(Johnson-Lindenstrauss Lemma): Let $\epsilon \in (0,1)$ and $D_g > 0$ be such that for any integer n, $D_g \geq 4 \left(\epsilon^2/2 - \epsilon^3/3\right)^{-1} \ln n$. Then, for any set of points $Z \in \mathbb{R}^{D_h}$, there exists a mapping function $\mathcal{M} : \mathbb{R}^{D_h} \to \mathbb{R}^{D_g}$ such that for all pairs of samples p, q*
$$(1-\epsilon)\|p - q\|^2 \leq \|\mathcal{M}(p) - \mathcal{M}(q)\|^2 \leq (1+\epsilon)\|p - q\|^2$$

Fundamentally, Theorem 2 proves that one can effectively reduce the dimensions of any $n \in \{1, 2, .., D_h\}$ points in a Euclidean subspace to $D_g = \mathcal{O}\left(\log n/\epsilon^2\right)$ dimensions without distorting the distances between n points more than $1 \pm \epsilon$. Magen (2002) further observed that the Johnson-Lindenstrauss lemma preserves any 'D_h-dimensional angle' by projecting down to dimension $\mathcal{O}\left(D_h \varepsilon^{-2} \log n\right)$. Therefore, it can be safely assumed that it is possible to transfer geometric structures in the projection head to the low-dimensional classifier's hypersphere without the loss of generality. To this end, we propose $\mathcal{L}_{ecr}$ as a mapping function to emulate the rich geometric structures learned within the hypersphere of the projection head to compensate for weak supervision in the classifier under low buffer regimes.

B   Broader Related Works

In section 2, we covered the most important baselines that can be compared and contrasted analytically. In this section, we explore broader related works whose problem statement overlaps with that of our proposed method.

The problem of inter-task class separation in Class-IL remains a significant challenge due to the difficulty in establishing clear boundaries between classes of current and previous tasks (Lesort et al., 2019). When a limited number of samples from previous tasks are available in the buffer, the CL model tends to overfit on the buffered samples and incorrectly approximates the class boundaries between classes from current and previous tasks. Kim & Choi (2021) splits the Class-IL problem into intra-old, intra-new and cross-task knowledge. The cross-task knowledge specifically addresses the inter-task class separation through knowledge distillation. Similarly, Kim et al. (2022) decomposes the Class-IL into two sub-problems: within-task prediction (WP) and task-id prediction (TP). Essentially, a good WP and good TP or out-of-distribution detection are necessary and sufficient for good Class-IL performance (Kim et al., 2022). On the other hand, some approaches propose to address inter-task forgetting without decomposition. Attractive and repulsive training (ART) (Choi & Choi, 2022), which effectively captures the previous feature space into a set of class-wise flags, and thereby makes old and new similar classes less correlated in the new feature space. LUCIR (Hou et al., 2019) incorporates cosine normalization, less-forget constraint, and inter-class separation, to mitigate the adverse effects of the imbalance in Class-IL. Although these approaches address fine grained problem of inter-task class separation in Class-IL, catastrophic forgetting is greatly reduced as a direct consequence.

Rehearsal-based approaches that store and replay previous task samples have been quite successful in mitigating forgetting across CL scenarios. These strategies, however, suffer from a common pitfall: as the memory buffer only stores a tiny portion of historical data, there is a significant chance that they may overfit, hurting generalization (Verwimp et al., 2021). Therefore, several methods resort to augmentation techniques either by combining multiple data points into one (Boschini et al., 2022) or by producing multiple versions of the same buffer data point (Bang et al., 2021). Gradient-based Memory EDiting (GMED) (Jin et al., 2021) proposes to create more "challenging" examples for replay by providing a framework for editing stored examples in continuous input space via gradient updates. Instead of individually editing memory data points without considering distribution uncertainty, Distributionally Robust Optimization (DRO) (Wang et al., 2022b) framework focuses on population-level and distribution level evolution. On the other hand, Lipschitz Driven Rehearsal (LiDER) (Bonicelli et al., 2022) proposes a surrogate objective that induces smoothness in the backbone network by constraining its layer-wise Lipschitz constants w.r.t. replay examples. As many of these approaches are intended to be orthogonal to the existing rehearsal-based approaches, they allow for seamless integration and effective reduction in memory overfitting in CL.

C CHARACTERISTICS ANALYSIS

C.1 FORGETTING ANALYSIS

Continually learning on a sequence of novel tasks often interferes with previously learned information resulting in catastrophic forgetting. Therefore, in addition to the average accuracy of the previous tasks, it is crucial to measure how much of the learned information is preserved. The forgetting measure (f_j^k) (Chaudhry et al., 2018) for a task j after learning k tasks is defined as the difference between the maximum knowledge gained for the task in the past and the knowledge currently in the model. Let A_{ij} be the test accuracy of the model for task j after learning task i then,

$$f_j^k = \max_{l \in \{j, j+1, .., k-1\}} A_{lj} - A_{kj}, \forall j < k \tag{8}$$

Then the average forgetting measure for the model after learning T tasks is given by

$$F_T = \frac{1}{T-1} \sum_{j=0}^{T-1} f_j^T \tag{9}$$

The lower F_T signifies less forgetting of previous tasks. Typically, A_{ij} is computed at the task boundary after learning the task i. However, since the EMA is updated stochastically, the maximum accuracy for a previous task is not necessarily achieved at the task boundaries. Therefore, we evaluate the EMA on previous tasks after every epoch and keep track of the maximum accuracy observed for the previous tasks. Forgetting analysis of IMEX-Reg is then computed with respect to the maximum accuracy observed for the previous tasks and the final evaluation accuracy for the tasks at the end of training.

Table 4 shows the average forgetting measures for different CL methods across different datasets and buffer sizes in a Class-IL setting. IMEX-Reg and OCDNet achieve significantly lower forgetting than other baselines, owing to the ability of the EMA to preserve the consolidated knowledge. In Seq-TinyImageNet, OCDNet suffers from far less forgetting than IMEX-Reg. However, this can be attributed to how often the EMA is updated. By restricting the update frequency of EMA, we can considerably reduce forgetting but at the cost of adapting to new information. An ideal CL model should not be too restrictive and instead should find an optimal balance between forgetting and learning novel tasks.

Table 4: Forgetting analysis for various CL models across datasets in Class-IL setting.

Buffer	Methods	Seq-CIFAR10	Seq-CIFAR100	Seq-TinyImageNet
200	ER	61.24±2.62	75.54±0.45	76.37±0.53
	DER++	32.59±2.32	68.77±1.72	72.74±0.56
	OCDNet	**22.63**±2.06	33.41±2.87	**20.37**±1.05
	IMEX-Reg	24.69±0.84	**32.19**±0.51	27.93±2.99
500	ER	45.35±0.07	67.74±1.29	75.27±0.17
	DER++	22.38±4.41	50.99±2.52	64.58±2.01
	OCDNet	**14.93**±1.42	21.6±0.16	**17.88**±0.55
	IMEX-Reg	17.00±0.40	**18.83**±0.51	30.47±0.35

C.2 STABILITY-PLASTICITY TRADE-OFF

While forgetting F_T quantifies how much knowledge is preserved in the model, we need to evaluate how well it is at adapting to novel tasks. The extent to which CL systems need to be plastic in order to acquire novel information and stable in order to retain existing knowledge is known as the stability-plasticity dilemma. There is an inherent trade-off between the plasticity and stability of the model, and estimating this trade-off can shed some light on this dilemma. Sarfraz et al. (2022) proposes a *Trade-off* measure that approximates the balance between the stability and plasticity of the model. After learning the final task T, the stability (S) of the model is estimated as the average performance of all previous $T - 1$ tasks.

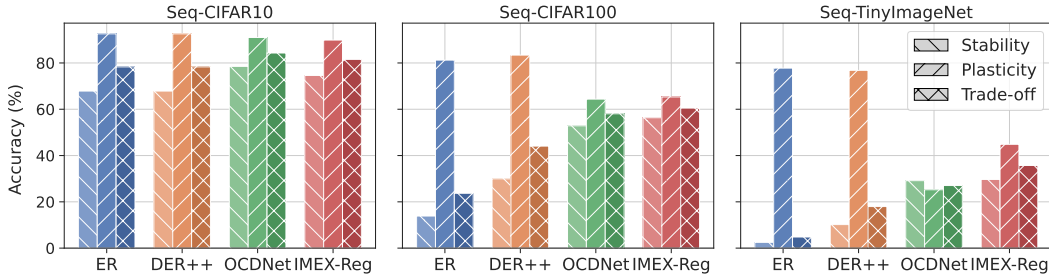$$S = \sum_{i=0}^{T-1} A_{Ti} \tag{10}$$

Figure 4: Comparison of Stability-Plasticity Trade-off for different CL models across different datasets.

The plasticity (P) of the model is measured as the average performance of each task after it is learned for the first time.

$$P = \sum_{i=0}^{T} A_{ii} \tag{11}$$

To find an optimal balance between the stability and plasticity of the model, Sarfraz et al. (2022) computes the harmonic mean of S and P as a trade-off measure, that is,

$$\textit{Trade-off} = \frac{2SP}{S + P} \tag{12}$$

Figure 4 compares the stability, plasticity, and trade-off of different CL methods across different datasets for a buffer size of 500. ER and DER++ have high plasticity and quickly adapt to novel information; yet, they do not retain previously learned information. On the other hand, IMEX-Reg and OCDNet employ an EMA that is stochastically updated and better preserves consolidated knowledge. Hence, both IMEX-Reg and OCDNet achieve much higher stability at a relatively lower cost of plasticity, resulting in a higher stability-plasticity trade-off. In Table 4, we see that OCDNet suffered the least forgetting in Seq-TinyImageNet. However, Figure 4 shows that OCDNet achieved the least plasticity in Seq-TinyImageNet. IMEX-Reg, on the other hand, achieved a much better trade-off, even though it forgets more than OCDNet.

C.3   MODEL CALIBRATION

CL systems deployed in the real world are expected to be reliable by exhibiting a sufficient level of prediction uncertainty. Expected Calibration Error (ECE) provides a good estimate of reliability by gauging the difference in expectation between confidence and accuracy (Guo et al., 2017). Figure 5 shows the comparison of our method with other baselines using a calibration framework (Küppers et al., 2020). Compared to other baselines, IMEX-Reg achieves the lowest ECE value and is considerably well calibrated. In addition to improving generalization, regularizing the classifier implicitly through the auxiliary CRL and explicitly in the function space by aligning with geometric structures learned in the projection head prevents the model from being overconfident.

C.4   TASK-WISE PERFORMANCE

To better understand how different tasks are learned, Figure 6 shows the task-wise performance of different CL methods during the course of training on Seq-CIFAR100 for a buffer size of 500. ER and DER++ clearly adapt quickly to new tasks, but knowledge is not preserved. Whereas by using a stochastically updated EMA, IMEX-Reg and OCDNet adapt fairly well to new tasks and preserve the learned information.

C.5   ADDITIONAL EXPERIMENTAL EVALUATION ON SEQ-CIFAR100

Table 5 provides Top-1 accuracy (%) of different CL models in Class-IL and Task-IL scenarios on Seq-CIFAR100 with 2, 5, and 10 tasks. As can be seen, IMEX-Reg performs extremely well in 2 and
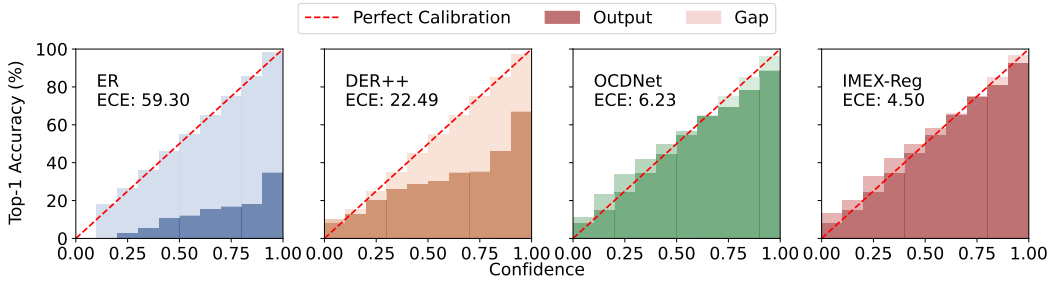
Figure 5: Reliability diagrams with Expected Calibration Error (ECE) for CL methods trained on Seq-CIFAR100 with 5 tasks. The lower ECE value signifies a better calibrated model. Compared to baselines, IMEX-Reg is well calibrated with the lowest ECE value.
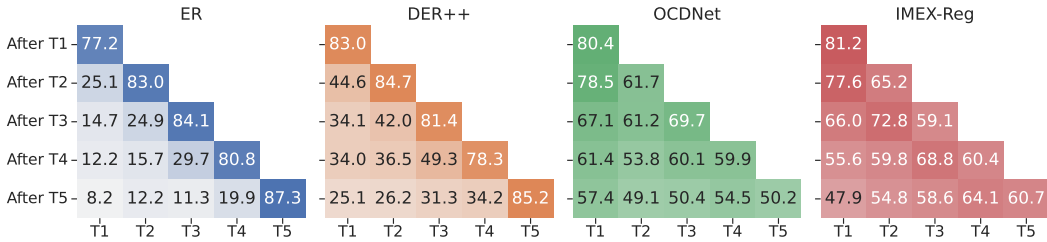

Figure 6: Task-wise performance for CL models trained on Seq-CIFAR100 with 5 tasks

5 tasks. It outperforms OCDNet by a relative 7.2% and 4.4% in Class-IL in these cases, respectively. However, in the case of 10 tasks, it lags behind OCDNet by a small margin, but not significantly. We speculate that this might be due to the inability of $\mathcal{L}_{ecr}$ to effectively capture geometric relationships under longer task sequences where the number of samples from previous tasks is heavily limited.

Table 5: Top-1 accuracy (%) of different CL models in Class-IL and Task-IL scenarios on Seq-CIFAR100 with 2, 5, and 10 tasks. Randomly initialized ResNet18 is used as a common backbone with buffer size of 500 for all these scenarios. The best results are marked in bold.

Methods	2 tasks		5 tasks		10 tasks	
	Class-IL	Task-IL	Class-IL	Task-IL	Class-IL	Task-IL
ER	44.77 ± 0.68	66.02 ± 0.07	28.02 ± 0.31	68.23 ± 0.17	21.54 ± 0.29	74.97 ± 0.91
DER++	49.68 ± 1.92	65.50 ± 1.76	41.40 ± 0.96	70.61 ± 0.08	36.15 ± 1.10	73.31 ± 0.78
OCDNet	60.44 ± 1.89	73.86 ± 0.91	54.13 ± 0.36	78.51 ± 0.24	$\mathbf{47.35 \pm 0.40}$	$\mathbf{83.5 \pm 0.37}$
IMEX-Reg	$\mathbf{64.82 \pm 0.19}$	$\mathbf{75.46 \pm 0.21}$	$\mathbf{56.53 \pm 0.80}$	$\mathbf{80.51 \pm 0.10}$	46.46 ± 1.15	82.69 ± 0.38

D LIMITATIONS, FUTURE WORK AND BROADER IMPACT

D.1 LIMITATIONS AND FUTURE WORK

IMEX-Reg is a two-pronged CL approach aimed at implicit regularization using hard parameter sharing and multitask learning, and a novel explicit regularization in the function space to guide the optimization of the CL model toward generalization. In addition to CRL and consistency regularization, IMEX-Reg entails a novel explicit classifier regularization to emulate rich geometric structures learned within the projection head hypersphere to compensate for weak supervision under low-buffer regimes. As IMEX-Reg involves many inductive biases to help improve the generalization performance in CL, it necessitates hyperparameter tuning to find the best combination of these biases. Furthermore, finding the right set of inductive biases for novel domains may not be trivial. In addition,

the selected inductive biases should be such that they complement each other and especially benefit CL.

As IMEX-Reg involves an auxiliary CRL, representation learning in the projection head could be further improved by leveraging the vast unlabeled data. Learning generic representations through unlabeled data could relax the need to store a large number of images in the buffer. We leave the extension of IMEX-Reg to other domains, and different CL scenarios, and enhancing with unlabeled data for future work.

D.2 BROADER IMPACT

We propose IMEX-Reg to improve the generalization performance of experience rehearsal in CL under low-buffer regimes. By leveraging hard parameter sharing, multitask learning, and explicit classifier regularization, IMEX-Reg enhances the ability of CL models to generalize well across tasks and adapt to new domains. This can lead to more robust and reliable AI systems in various real-world applications. In addition, the CRL in IMEX-Reg opens up opportunities to leverage unlabeled data for learning generic representations, reducing the reliance on large labeled datasets. By enabling models to learn continuously and adapt to new tasks, IMEX-Reg contributes to the responsible and ethical deployment of AI technologies, as models can continuously improve and update their knowledge without requiring extensive retraining.

E IMPLEMENTATION DETAILS

E.1 CONTINUAL LEARNING SETTINGS

We evaluate the performance of our method in three different CL settings, namely, Task Incremental Learning (Task-IL), Class Incremental Learning (Class-IL), and General Continual Learning (GCL).

In Task-IL and Class-IL, each task consists of a fixed number of novel classes that the model must learn. A CL model learns several tasks sequentially while distinguishing all classes it has seen so far. Task-IL is very similar to Class-IL, with the exception that task labels are also available during inference, making it the easiest scenario. Although Class-IL is a widely studied and relatively harder CL setting, it makes several assumptions that are realistic, such as a fixed number of classes in each task and no reappearance of classes. (Mi et al., 2020). GCL relaxes such assumptions and presents more challenging real-world-like scenarios where the task boundaries are blurry and classes reappear with different distributions.

E.2 DATASETS

For Task-IL and Class-IL scenarios, we obtain Seq-CIFAR10, Seq-CIFAR100, and Seq-TinyImageNet by splitting CIFAR10, CIFAR100, and TinyImageNet into 5, 5, and 10 tasks of 2, 20, and 20 classes, respectively. The three datasets present progressively challenging scenarios (increasing the number of tasks or number of classes per task) for a comprehensive analysis of different CL methods. Generalized Class-IL (GCIL) (Mi et al., 2020) exposes the model to a more challenging scenario by utilizing probabilistic distributions to sample data from the CIFAR100 dataset in each task. The CIFAR100 dataset is split into 20 tasks, with each task containing 1000 samples with a maximum of 50 classes. GCIL provides two variations for sample distribution, Uniform and Longtail (class imbalance). GCIL is the most realistic scenario with varying numbers of classes per task and classes reappearing with different sample sizes.

E.3 MODEL AND TRAINING

We use the same backbone as recent approaches in CL (Buzzega et al., 2020; Arani et al., 2022), i.e., a ResNet-18 backbone without pre-training for all experiments. We use a linear layer, 3-layer MLP with BatchNorm and ReLu, and 2-layer MLP for the classifier, projection head, and classifier projection, respectively.

To ensure uniform experimental settings, we extended the Mammoth framework (Buzzega et al., 2020) and followed the same training scheme such as the SGD optimizer, batch size, number of

Table 6: The best hyperparameters for IMEX-Reg to reproduce the results reported in Table 1

Dataset	Buffer	LR	Epochs	γ	η	α	β	λ
Seq-CIFAR10	200	0.03	50	0.4	0.999	0.1	0.1	0.3
	500	0.03	50	0.4	0.999	0.1	0.2	0.3
Seq-CIFAR100	200	0.03	50	0.08	0.999	0.1	0.3	0.15
	500	0.03	50	0.08	0.999	0.1	0.2	0.15
Seq-TinyImageNet	200	0.03	20	0.1	0.999	0.1	0.1	0.2
	500	0.03	20	0.15	0.999	0.1	0.1	0.3
GCIL100 Uniform	100	0.03	100	0.1	0.999	0.2	0.2	0.15
	200	0.03	100	0.1	0.999	0.2	0.2	0.15
	500	0.03	100	0.1	0.999	0.2	0.2	0.15
GCIL100 Longtail	100	0.03	100	0.1	0.999	0.2	0.2	0.15
	200	0.03	100	0.1	0.999	0.2	0.2	0.15
	500	0.03	100	0.1	0.999	0.2	0.2	0.15

training epochs, and learning rate for all experiments, unless otherwise specified. We employ random horizontal flip and random crop augmentations for supervised learning in Seq-CIFAR10, Seq-CIFAR100, Seq-TinyImageNet, and GCIL-CIFAR100 experiments. For the contrastive representation learning in projection head, we transform the input batch using a stochastic augmentation module consisting of random resized crop, random horizontal flip followed by random color distortions. We trained all our models on NVIDIA's GeForce RTX 2080 Ti (11GB). On an average, it took around 2 hours to train IMEX-Reg on Seq-CIFAR10 and Seq-CIFAR100, and approximately 8 hours to train on Seq-TinyImageNet.

E.4 RESERVOIR SAMPLING

Algorithm 2 provides the steps for the reservoir sampling strategy (Vitter, 1985) for maintaining a fixed-size memory buffer from a data stream. Each sample in the data stream is assigned an equal probability of being represented in the memory buffer. When the buffer is full, sampling and replacement are performed at random, without assigning any priority to the samples that are added or replaced.

Algorithm 2 Reservoir sampling (Vitter, 1985)

Input: Data streams $\mathcal{D}_t$, Memory Buffer $\mathcal{D}_m$, Maximum buffer size $\mathcal{M}$, Number of seen samples $\mathcal{N}$,
Current sample $\{x, y\} \in \mathcal{D}_t$
if $\mathcal{M} > \mathcal{N}$ **then**
    $\mathcal{D}_m[\mathcal{N}] \leftarrow \{x, y\}$
else
    $i = randomInteger(min = 0, max = \mathcal{N})$
    if $i < \mathcal{M}$ **then**
        $\mathcal{D}_m[i] \leftarrow \{x, y\}$
return $\mathcal{D}_m$

E.5 HYPERPARAMETERS

Table 6 provides the best hyperparameters used to report the results in Table 1. In addition to these hyperparameters, we use a standard batch size of 32 and a minibatch size of 32 for all our experiments.

E.6 HYPERPARAMTER TUNING

Table 7: Hyperparamter tuning for IMEX-Reg on Seq-CIFAR100 with buffer size 200. As can be seen, IMEX-Reg is quite robust to choice of hyperparameters.

Varying α, for $\beta = 0.3, \lambda = 0.15$		Varying β, for $\alpha = 0.1, \lambda = 0.15$		Varying λ, for $\alpha = 0.1, \beta = 0.3$	
α	Top-1 Acc %	β	Top-1 Acc %	λ	Top-1 Acc %
0.05	47.72	0.1	48	0.1	48.07
0.1	**48.54**	0.2	47.95	**0.15**	**48.54**
0.2	47.90	**0.3**	**48.54**	0.2	47.4
0.3	47.26	0.4	48.06		